

Characterization of Actinide Bonding in $\text{Th}(\text{S}_2\text{PMe}_2)_4$ by Synchrotron X-ray Diffraction

Bo B. Iversen,^{*,†} Finn K. Larsen,[†] Alan A. Pinkerton,[‡] Anthony Martin,[‡]
Alexander Darovsky,[§] and Philip A. Reynolds^{||}

Department of Chemistry, University of Aarhus, DK8000 Aarhus C, Denmark,
Department of Chemistry, University of Toledo, Toledo, Ohio 43606, National Synchrotron Light
Source, Brookhaven National Laboratory, Upton, New York 11973, and Research School of Chemistry,
Australian National University, Canberra, ACT 0200, Australia

Received December 11, 1997

Extensive synchrotron (28 K) and conventional sealed-tube (9 K) X-ray diffraction data have been collected on $\text{Th}(\text{S}_2\text{PMe}_2)_4$. Modeling of the electron density of the complex shows the bonding is quite ionic with little diffuse f or d type bonding density. Furthermore a large polarization of the Th core is observed revealing some 5d-like involvement in the bonding. High-quality ab initio density functional calculations are not able to reproduce these features and instead predict rather covalent bonding with considerable 6d–5f mixing. The study suggests that this theoretical method exaggerates the covalent nature of actinide bonds. It is shown that the most direct measure of covalence—charge transfer and electron distributions—can be usefully estimated by X-ray diffraction even in this most unfavorable of cases, where many actinide core electrons are present. The use of very low temperature data is crucial in the study of heavy metal complexes in order to minimize systematic errors such as thermal diffuse scattering and anharmonicity. The fact that accurate synchrotron radiation diffraction data can be measured within days makes studies of compounds beyond the first transition series more frequently within reach.

1. Introduction

Bonding in complexes involving heavy metals has been little studied by X-ray diffraction methods. Apart from a number of simple salts—oxides, halides, borides, phosphides—we believe there are no accurate studies of compounds involving lanthanides or heavier metals. This is a result of a number of factors. First, their chemistry is less well-known than that for the first transition series of metals, simple complexes are less common, and the growth of large single crystals is generally more difficult. For X-ray diffraction, unlike polarized neutron diffraction, there is in general the additional serious difficulty of the large number of metal core electrons swamping those electron density changes due to bonding effects. Nevertheless, such studies are attractive because the bonding between heavy metals and relatively complex ligands is not well understood, particularly since it involves many energetically closely spaced atomic functions and relativistic effects cannot be ignored.

There has been much debate about the role of the 5f electrons in the bonding in actinide complexes¹ as well as about the relative ionic and covalent bonding contributions in actinide and lanthanide complexes.² Simple considerations of f-orbital spatial extent would lead us to predict the greatest covalence for low-oxidation-state early actinide complexes. Adequate theoretical calculations on actinide complexes are difficult and therefore sparse in the literature. In the calculations that have been carried out, it is generally found that the bonding contains considerable

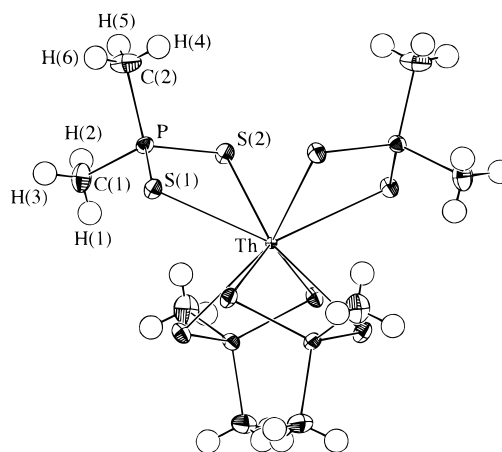


Figure 1. ORTEP drawing of $\text{Th}(\text{S}_2\text{PMe}_2)_4$ showing 90% thermal ellipsoids and the atom numbering scheme. The projection shows the *ac* plane.

covalent contributions with significant 5f involvement, even in a U(IV) complex.³ Direct experimental testing of this picture is clearly desirable.

The structure of $\text{Th}(\text{S}_2\text{PMe}_2)_4$, Figure 1, is attractive for an accurate study by X-ray diffraction because it contains a thorium–sulfur bond likely to be a real test for theoretical studies. The study has some hope of success since the crystal structure is unusually simple and symmetrical for a heavy metal complex. A search of the Cambridge Crystallographic Data File produced only a handful of chemical complexes involving second transition series, or heavier, metals with fewer than 10 unique non-hydrogen atoms. This complex involves only six non-hydrogen and six hydrogen unique atoms, a neutral

* To whom correspondence should be addressed. E-mail: bo@kemi.aau.dk.
Fax: +45-86196199.

[†] University of Aarhus.

[‡] University of Toledo.

[§] Brookhaven National Laboratory.

^{||} Australian National University.

(1) Bursten, B. E.; Strittmatter, R. J. *Angew. Chem., Int. Ed. Engl.* **1991**, *30*, 1069.

(2) Adamo, C.; Maldivi, P. *Chem. Phys. Lett.* **1997**, *268*, 61.

(3) Chang, A. A. H.; Pitzer, R. M. *J. Am. Chem. Soc.* **1989**, *111*, 2500.

molecule of D_2 symmetry,⁴ in a crystal of tetragonal symmetry. Crucially, half of the reflections contain *no* contribution from the spherical component of the electron-rich thorium core. Thus these reflections may provide good data concerning the ligand electron distribution, relatively unaffected by the heavy metal core. The previous published study was directed toward structure determination, being based on room-temperature data and being of low resolution, but it gave an encouraging agreement factor of 0.03 for $R(F)$.⁴ Our subsequent unpublished studies at higher resolution, both at room temperature and at liquid nitrogen temperatures, gave improved agreement and caused us to commence the study described in this paper. Clearly, for a charge density study, we will need the very best data currently available obtained at low temperatures. We have demonstrated the improvements obtainable in the copper Tutton salt, $(\text{ND}_4)_2\text{Cu}(\text{SO}_4)_2 \cdot 6\text{D}_2\text{O}$,⁵ and in tetraamminedinitronickel, $\text{Ni}(\text{ND}_3)_4(\text{NO}_2)_2$,⁶ by such a reduction in temperature. Such data can be directly compared to theory, with far less uncertainty due to the reduced effects of thermal motion at these low temperatures.⁷ Recently, Koritzansky et al.⁸ reported a synchrotron study of a simple organic molecule based on CCD data at 100 K. However, for studies of heavy metal coordination complexes, low temperatures, well below those obtainable by nitrogen-cooled devices, are necessary to reduce thermal motion and minimize both anharmonic and thermal diffuse scattering effects. This involves considerable extra experimental effort, since commercial CCD systems with liquid-nitrogen cooling are inadequate. Throughout this paper, we will use the term "accurate" in the statistical sense, that is, accuracy as opposed to precision. While liquid-nitrogen studies with CCD detectors are precise, lowering of the temperature is imperative to achieve accurate data free of systematic errors.

Here we have obtained data with both a conventional X-ray source and a synchrotron. The wavelengths used are lower than that of Mo $K\alpha$ radiation, since for this thorium-containing compound we need, more urgently than for lighter metals, to minimize both absorption corrections and anomalous dispersion effects. While a large number of electron density (ED) determinations have been reported on the basis of conventional X-ray data, so far very few accurate ED's have been reported on the basis of synchrotron data. This is primarily because of the very long data collection time for sequential mode measurements (1–2 months for typical small-molecule structures). It has been imperative to develop fast accurate area detector techniques in order to harvest the advantages of the large intensities and short wavelengths available at synchrotron sources. The present study demonstrates that fast, accurate area detector measurements now can be carried out at synchrotron sources. This greatly enhances the feasibility of experimental ED investigations. Below, we shall investigate how much bonding information can actually be obtained from $\text{Th}(\text{S}_2\text{PMe}_2)_4$ with the best current data. To assist in this, we have also used the results of good-quality ab initio quantum mechanical calculations. In a companion paper, we discuss in detail the novel experimental procedures and data reduction techniques and scrutinize the structural results.⁹

Table 1. Crystal Data, Experimental Details, and Structure Refinement Parameters for $\text{Th}(\text{S}_2\text{PMe}_2)_4$

radiation	sealed tube Ag $K\alpha$	synchrotron
temp/K	9(1)	28(5)
crystal size/mm	octahedron 0.076 mm face to face	octahedron 0.076 mm face to face, corner off
empirical formula	$\text{C}_8\text{H}_{24}\text{P}_4\text{S}_8\text{Th}$	$\text{C}_8\text{H}_{24}\text{P}_4\text{S}_8\text{Th}$
fw	732.7	732.7
$F(000)/e$	694.7	698.9
crystal system	tetragonal	tetragonal
space group	$P4_22_12$	$P4_22_12$
Z	2	2
$D_c/\text{Mg m}^{-3}$	1.92	1.90
μ/mm^{-1}	5.35	2.23
transm	0.42–0.49	0.72–0.76
$a/\text{\AA}$	10.386(1)	10.420(4)
$c/\text{\AA}$	11.742(2)	11.784(8)
$V/\text{\AA}^3$	1266.6(4)	1279(1)
wavelength/	0.5603	0.394(2)
2θ range/deg	0 → 46.0, 60 → 64	0 → 44 (low) 11 → 87.8 (high)
no. of reflns collected	5826	81 185 (low) 38 969 (high)
no. of unique reflns	2529	3677 (low) 12 671 (high)
$R(\text{int})$	0.028	0.050 (low) 0.017 (high)
GOF on F^2	1.14	0.83 (low) 1.89 (high)
$R(F)$ [$F^2 > 3\sigma(F^2)$]	0.022	0.011 (low) 0.030 (high)
$R(F^2)$ (all data)	0.033	0.014 (low) 0.042 (high)
$R_w(F^2)$ (all data)	0.055	0.023 (low) 0.061 (high)

2. Experimental Section

2.1. X-ray Data Modeling. Three separate sets of unique X-ray data (a conventional X-ray tube set, a high-order synchrotron set, and a low-order synchrotron set) were collected. A detailed account of the data collection and reduction can be found elsewhere.⁹ The data collection involves use of a Displex refrigerator fitted with a Darovsky antiscatter device to block out parasitic scattering from the vacuum chamber.¹⁰ Data reduction was performed with the seed-skewness integration routine, which has been shown to extract weak intensities well.¹¹ Table 1 is a summary of some of the experimental details and crystal data. The three separate sets of unique X-ray data (the tube and the high- and low-order synchrotron datasets) were refined using the ASRED program.¹² The observations were fitted to a harmonic model of nuclear position and displacement and a multipole model of the electron density which is described in more detail below. We also included simplified corrections for multiple scattering and type II extinction, a method described in more detail elsewhere, e.g. by Figgis et al.⁵ Since $h + k + l$ odd and $h + k + l$ even reflections are on average very different in intensity, due to the difference in thorium contributions, we may expect differences in multiple scattering, and therefore separate $h + k + l$ odd and $h + k + l$ even multiple-scattering parameters were refined. The quantity $\sum\{\sigma(F^2)^{-2}[F_o^2 - F_c^2]^2\}$ was minimized until a maximum shift/esd of 0.1 was obtained.

The positional parameters of all 12 unique atoms were refined, by starting from the values of the original structure determination and

(4) Pinkerton, A. A.; Storey, A. E.; Zellweger, J.-M. *J. Chem. Soc., Dalton Trans.* **1981**, 1475.

(5) Figgis, B. N.; Iversen, B. B.; Larsen, F. K.; Reynolds, P. A. *Acta Crystallogr., Sect. B* **1993**, *49*, 794.

(6) Iversen, B. B.; Larsen, F. K.; Figgis, B. N.; Reynolds, P. A. *J. Chem. Soc., Dalton Trans.* **1997**, 2227.

(7) Chandler, G. S.; Figgis, B. N.; Reynolds, P. A.; Wolff, S. K. *Chem. Phys. Lett.* **1994**, *225*, 421.

(8) Koritzansky, T.; Flaig, R.; Zobel, D.; Krane, H.-G.; Morgenroth, W.; Luger, P. *Science* **1998**, *279*, 356.

(9) Iversen, B. B.; Larsen, F. K.; Pinkerton, A. A.; Martin, A.; Darovsky, A.; Reynolds, P. A. *Acta Crystallogr., Sect. B*, in press.

(10) Darovsky, A.; Bolotovskiy, R.; Coppens, P. *J. Appl. Crystallogr.* **1994**, *27*, 1039.

(11) (a) Bolotovskiy, R.; White, M.; Darovsky, A.; Coppens, P. *J. Appl. Crystallogr.* **1995**, *28*, 86. (b) Bolotovskiy, R.; Coppens, P. *J. Appl. Crystallogr.* **1997**, *30*, 65. (c) Darovsky, A.; Kezerashvili, V. *J. Appl. Crystallogr.* **1995**, *30*, 128.

(12) Figgis, B. N.; Reynolds, P. A.; Williams, G. A. *J. Chem. Soc., Dalton Trans.* **1980**, 2339.

interpolated hydrogen positions using known methyl group geometry.⁴ We refined only isotropic harmonic displacement parameters for the hydrogens but anisotropic harmonic displacement parameters for the heavy atoms. Anomalous dispersion corrections were calculated for thorium and the other heavy atoms.¹³ We note that the calculated values for silver radiation for thorium ($f' = -3.74$, $f'' = 9.89$) are substantially larger than those for the synchrotron wavelength ($f' = -1.04$, $f'' = 5.64$).

The valence model for the charge density consisted of atom-centered functions. Core electron density functions on the heavy atoms and valence distributions on all atoms were obtained from a standard compilation¹⁴ or by use of the program JCALC¹⁵ with Hartree-Fock atomic wave functions.¹⁶ The valence functions on Th consisted of the difference of Th and Th⁴⁺ form factors, i.e., the $6d^{27}s^2$ form factor together with some small core rearrangement, with angular variation up to fourth-order multipoles. In addition, we added a more contracted set, arbitrarily chosen with Tc 4d radial dependence,¹⁷ again with angular dependence up to fourth order. On S, P, and C centers, since both molecular changes and atomic calculations are more reliable than those for Th, less flexibility is required. We placed 3p, 3p, and 2p radial dependence, with angular variation to third order on S, P, and C, respectively, and a spherical 1s-like distribution on H.¹⁸ The radial extent of all the valence functions was allowed to vary in the usual κ refinement,¹⁹ and all valence populations were allowed to vary. Because of uncertainty in the relativistic treatment of the atomic calculation for such a heavy atom as thorium, the core radius was also allowed to vary in the κ manner. In addition, Gaussian densities of width 0.16 Å² were placed in the six independent bond midpoints between non-hydrogen atoms to help model bond overlap density, and the populations of these were refined. The unit cell content of electrons was constrained to the formula number.

Since the thorium atom is very heavy and the spherical component of the core contributes to only half of the reflections, whose intensities it tends to dominate, its charge becomes more uncertain than those for other atom sites. The refined value of the thorium charge becomes dominated by the relative scale factors of $h + k + l$ even and $h + k + l$ odd reflections. This ratio in turn has systematic errors due to the different effects of multiple scattering in the strong $h + k + l$ even and weaker $h + k + l$ odd data and the effect of extinction. Since Th⁰ has 90 electrons, to define its charge to chemical accuracy requires knowledge of the scale factors and extinction corrections to better than 1%. We have, therefore, in the tube data and the high-order synchrotron datasets constrained the thorium charge to +1, a value consistent with the ADF ab initio calculation and general chemical expectations arising from Pauling's principle of electroneutrality. We should note that we later determined that this generally acceptable assumption may not in fact be correct. The low-order synchrotron dataset contains sufficient low-angle data of sufficient accuracy to attempt to refine the Th site total charge.

While the ligand densities in any model are defined quite well by the $h + k + l$ odd data alone, there are many aspherical components on the thorium site defined only by the $h + k + l$ even data. Of the d-type distributions only the difference of d_{xz} and d_{yz} are defined by the $h + k + l$ odd data— d_z^2 , $d_{x^2-y^2}$, d_{xy} , and $(d_{xz} + d_{yz})$ are all fixed by the $h + k + l$ even data. However, such anisotropic terms are much less affected than the total charge by scale factor errors. This is because, in terms of the ratio of the error to the fitted values, useful chemical information is obtained with much poorer relative definition of the values. While in the refinement we notice that spherical (monopole)

Table 2. Observed Geometry of the Th(S₂PMe₂)₄ Molecule in the Crystal (First Entry) and That Calculated by the ADF Method for the Free Molecule (Second Entry)

Bond Lengths (Å)					
Th-S(1)	2.9102(4)	3.039	C(1)-H(1)	0.77(5)	1.096
Th-S(2)	2.8787(4)	2.965	C(1)-H(2)	0.84(4)	1.099
P-S(1)	2.0114(5)	2.050	C(1)-H(3)	0.89(4)	1.099
P-S(2)	2.0127(5)	2.058	C(2)-H(4)	0.88(4)	1.098
C(1)-P	1.802(2)	1.843	C(2)-H(5)	0.86(4)	1.098
C(2)-P	1.803(2)	1.841	C(2)-H(6)	0.85(4)	1.098
Dihedral Angles (deg)					
H(1)-C(1)-P-C(2)		-185(1)			-181
H(2)-C(1)-P-C(2)		65(2)			60
H(3)-C(1)-P-C(2)		-58(2)			-61
H(4)-C(2)-P-C(1)		185(2)			180
H(5)-C(2)-P-C(1)		-54(2)			-60
H(6)-C(2)-P-C(1)		70(3)			61
Bond Angles (deg)					
S(1)-Th-S(2)		69.60(1)			69.68
S(1)-Th-S(1) ^I		132.86(1)			120.59
S(1)-Th-S(2) ^I		79.54(1)			73.76
S(1)-Th-S(1) ^{II}		67.70(1)			69.21
S(1)-Th-S(2) ^{II}		137.20(1)			133.89
S(1)-Th-S(1) ^{III}		134.37(1)			147.79
S(1)-Th-S(2) ^{III}		78.25(1)			86.19
S(2)-Th-S(2) ^I		96.98(1)			101.53
S(2)-Th-S(2) ^{II}		153.19(1)			155.74
S(2)-Th-S(2) ^{III}		89.20(2)			83.60
Th-S(1)-P		89.02(1)			87.26
Th-S(2)-P		89.89(2)			89.15
S(1)-P-S(2)		110.38(2)			113.23
S(1)-P-C(1)		110.50(6)			109.42
S(1)-P-C(2)		109.58(6)			110.37
S(2)-P-C(1)		108.96(6)			108.26
S(2)-P-C(2)		110.85(6)			110.23
C(1)-P-C(2)		106.50(9)			104.98

terms are only slightly correlated with aspherical (higher multipole) terms, it is well-known that an indirect connection can be observed through poor treatment of extinction and absorption. However, this is unlikely here since both are relatively isotropic and not large. Thus, ligand terms as well as aspherical terms on the thorium are well defined by these data.

The agreement factors are listed in Table 1 for the three data sets. The derived structure is discussed in ref 9. The molecular geometry is presented in Table 2. Figure 1 shows the molecular geometry, and Figure 2 shows the unit cell.

The anomalous dispersion from the Th sites is large, and so, for the low-order synchrotron dataset and the tube dataset, we performed a refinement with both real and anomalous parts refining. The anomalous dispersion remained at the calculated values, within 1σ , with errors in both of ca. 0.4 e. In subsequent refinements, these values were fixed at calculated values. Extinction effects in the refinements were small. Since the data extend very far in reciprocal space, it is possible to separate anharmonic thermal motion from electron deformation effects even with only a single-temperature X-ray data set at hand. A discussion of this aspect is provided in a companion paper.⁹

2.2. Electron Density and Bonding. The experimental deformation density is produced by subtracting from the observed electron density that of a promolecule composed of a superposition of free atom densities. It is thus a measure of the change in electron density on molecule formation followed by assembly of the crystal. The observed density is estimated by using a Fourier summation of $|F_o|$ with phases estimated from the best-model calculation and the promolecule density is calculated exactly, but both to a resolution given by $(\sin \theta)/\lambda < 0.7$ Å⁻¹ to minimize noise from higher angle data containing errors but little valence information. The residual density uses $(|F_o| - |F_{model}|)$ phased with model phases. The model deformation density is the difference of the experimental deformation and residual densities. The two types of deformation densities are found to be dominated by the apparent radial change in core density on the thorium. Figure 3 shows a typical section through the Th site and illustrates typical truncation

- (13) Brennan, S.; Cowan, P. L. *Rev. Sci. Instrum.* **1992**, *63*, 850.
 (14) *International Tables for X-ray Crystallography*; Kluwer Academic Publishers: Dordrecht, The Netherlands, 1992; Vol. C.
 (15) Figgis, B. N.; Reynolds, P. A.; White, A. H. *J. Chem. Soc., Dalton Trans.* **1987**, 1737.
 (16) Clementi, E.; Roetti, C. *At. Data Nucl. Data Tables* **1974**, *14*, 177.
 (17) Reynolds, P. A.; Figgis, B. N.; Forsyth, J. B.; Tasset, F. *J. Chem. Soc., Dalton Trans.* **1997**, 1447.
 (18) Stewart, R. F.; Davidson, E. R.; Simpson, W. T. *J. Chem. Phys.* **1965**, *42*, 3175.
 (19) Coppens, P.; Guru-Row, T. N.; Leung, P.; Stevens, E. D.; Becker, P.; Yang, Y. W. *Acta Crystallogr., Sect. A* **1979**, *35*, 63.

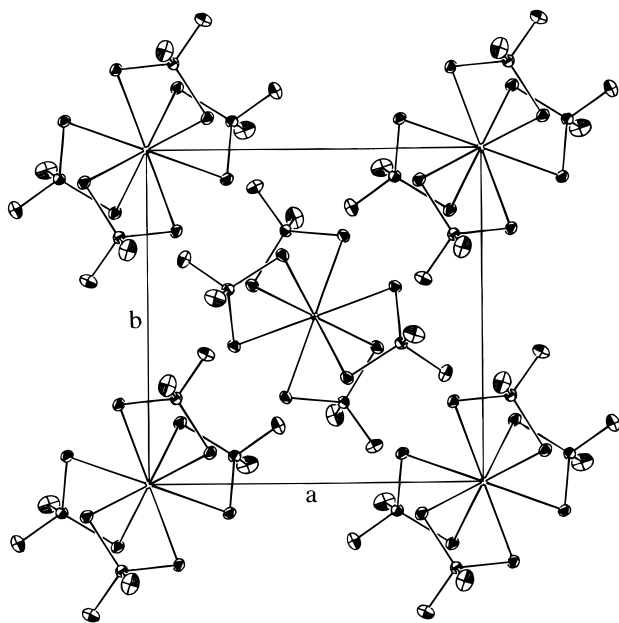


Figure 2. Unit cell contents in *ab* projection.

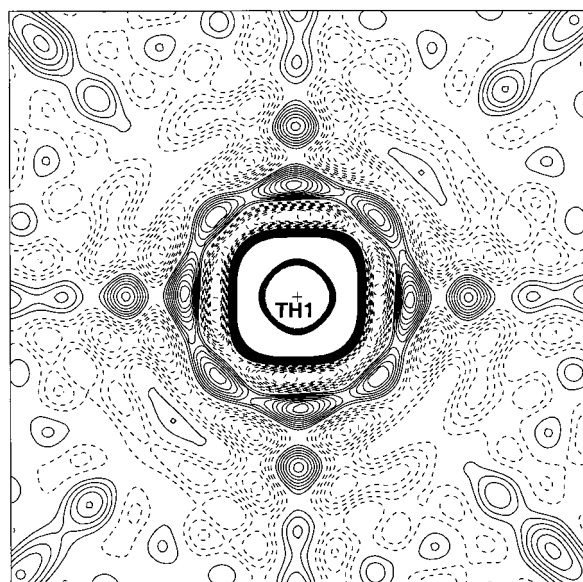


Figure 3. Experimental deformation density around the thorium site in the Th-S(1)-P plane. The contour interval is $0.1 \text{ e } \text{\AA}^{-3}$, the same in all subsequent diagrams, and the resolution is 0.7 \AA^{-1} . Very low and high level contours are both suppressed.

errors giving oscillation in the deformation density. Since this is a spherical term centered on the Th site, it is the least reliable effect and obscures other better estimated information (aspherical features on thorium and ligand information). Accordingly, we have recalculated the promolecule density incorporating the 3.3(5)% expansion modeled on the Th core in the Th atom density. All subsequent deformation maps are of this type. Since the model deformation maps are virtually identical to the experimental deformation, as testified in the very low residuals, we only show the experimental maps. Figures 4–8 show the experimental deformation densities as well as residual densities for the five most useful planes. These are two perpendicular sections through the Th atom (planes (001) and (110) and three planes through the ligand molecule (ThS₂, S₂P, PC₂). Figure 9 shows the experimental deformation density in a plane containing S(1) and S(2) perpendicular to the ThS₂ plane. There are no planes deliberately displaying hydrogen since our maps are derived from X-ray, not neutron, data and the hydrogen coordinates do not reflect the true proton positions. This also means that only the net charge of the methyl group as a whole

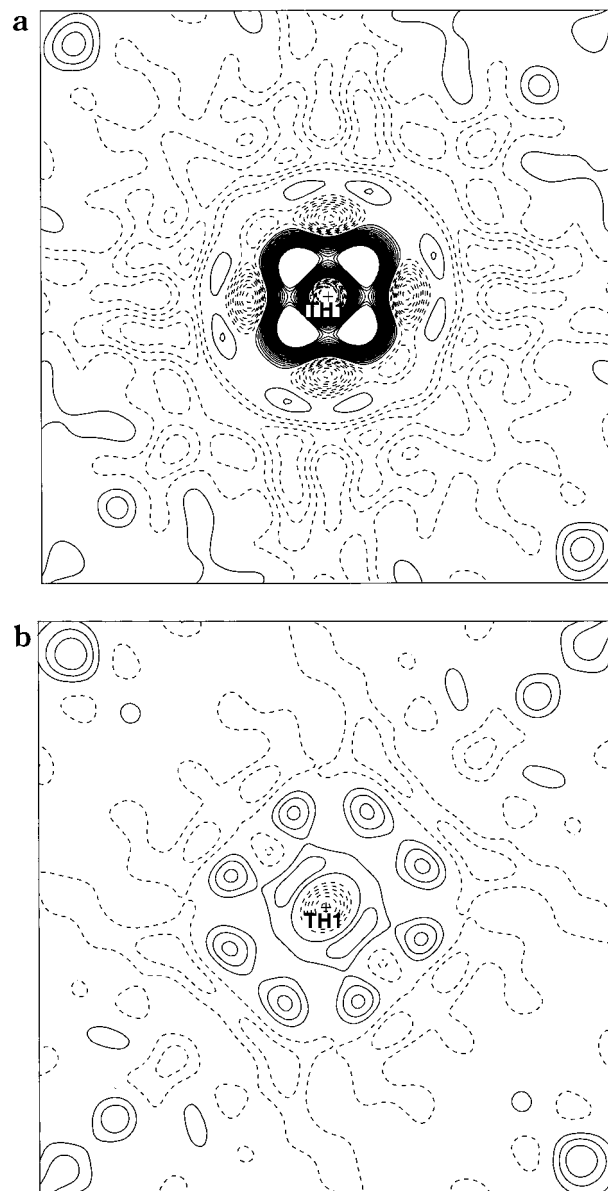


Figure 4. (a) Adjusted experimental deformation density. (b) Residual density in the (001) plane around the Th site.

can be estimated, and we have no information on C-H bond electron deformations relative to the nuclei. Net charges, derived from the modeling, are given in Table 3. The charges in the midbond parameters are divided equally, in the Mulliken fashion, between the bonded atoms. Their refined values are as follows (e): Th-S(1), 0.25(6); Th-S(2), 0.22(6); S(1)-P, 0.37(10); S(2)-P, 0.45(11); P-C(1), 0.95(14); P-C(2), 0.72(14).

2.3. Ab Initio Calculations. We performed calculations using the Amsterdam Density Functional (ADF) package²⁰ for the Th(S₂PM₂)₄ molecule in *D*₂ symmetry. These used a wave function with the Vosko-Wilks-Nusair local density approximation, Becke-Perdew gradient correction, and frozen relativistic atomic cores. We used the atomic bases Dirac Th.5d, S.2p, P.2p, C.1s, and H in which relativistic core pseudopotentials are generated from atomic solutions for cores extending to 5d for Th, 2p for S and P, and 1s for C. The remaining valence electrons are fitted using a Slater-type basis of approximately triple- ζ quality. The complete molecular geometry was optimized for the ¹A ground state using internal molecular coordinates as the variables,

(20) (a) Fonseca Guerra, C. *Methods and Techniques in Computational Chemistry*; Clementi, E., Corongiu, G., Eds.; STEF: Cagliari, Italy, 1995. (b) te Velde, G.; Baerends, E. J. *J. Comput. Phys.* **1992**, *99*, 84. (c) Baerends, E. J.; Ellis, D. E.; Ros, P. *Chem. Phys.* **1973**, *2*, 41.

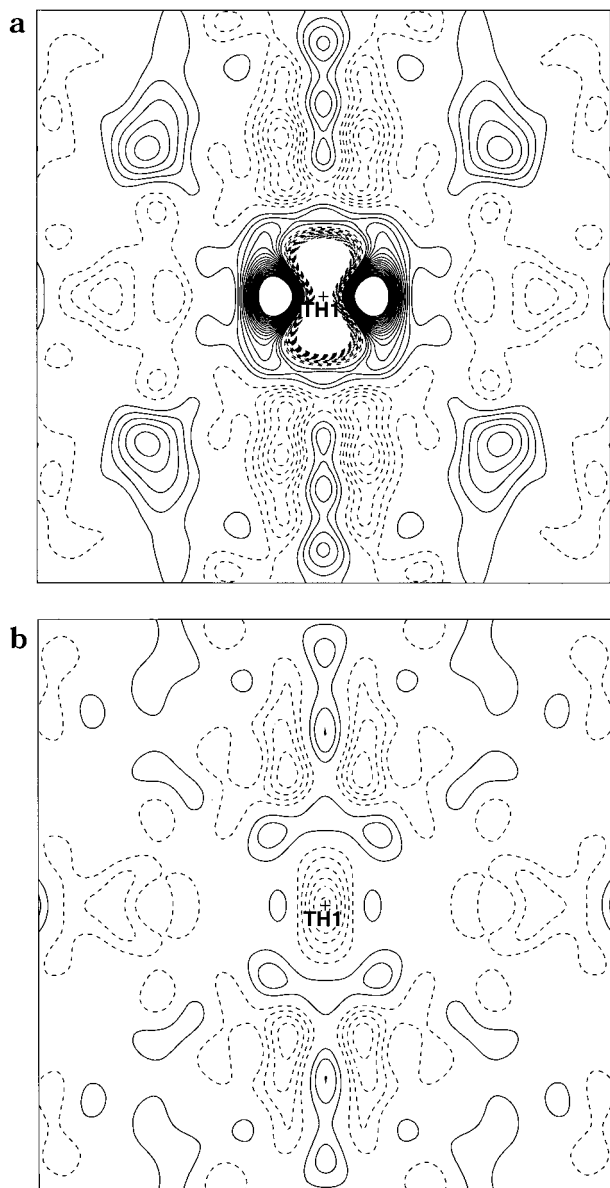


Figure 5. (a) Adjusted experimental deformation density. (b) Residual density in the (110) plane around the Th site.

in three stages of successively increasing internal molecular freedom, the last complete. Methyl torsions were then adjusted by $+60$ and -60° , and reoptimization was continued to check for local minima in this soft internal coordinate. The optimized molecular geometry is given in Table 2, and the Mulliken atomic populations are listed in Table 3. We obtain a converged total energy of $-8.695\,596\,97$ au. Similar calculations were also made for (a) the free dimethyldithiophosphinate (1 $-$) ligand, (b) four ligands assembled in the final molecular geometry, and (c) four ligands in the final molecular geometry with a point $+4$ electronic charge placed at the origin. Throughout the rest of this paper, we shall not discuss relativistic effects, taken into account here only indirectly through the relativistic effective core potentials, although this is probably rather a drastic neglect.

3. Results and Discussion

3.1. Molecular Geometry and Displacements. The thorium coordination, as discussed by Pinkerton et al.,⁴ involves an almost $D_{2d}(m\bar{m}m\bar{m})$ dodecahedral coordination. θ_A and θ_B angles have been used to discuss 8-fold bidentate coordination by Kepert.²¹ These have values of 61.7 and 25.5° for a perfect dodecahedron, contrasted with 67.5 and 22.5° for the nearest square antiprism. We observe 65.0 and 25.0° and calculate

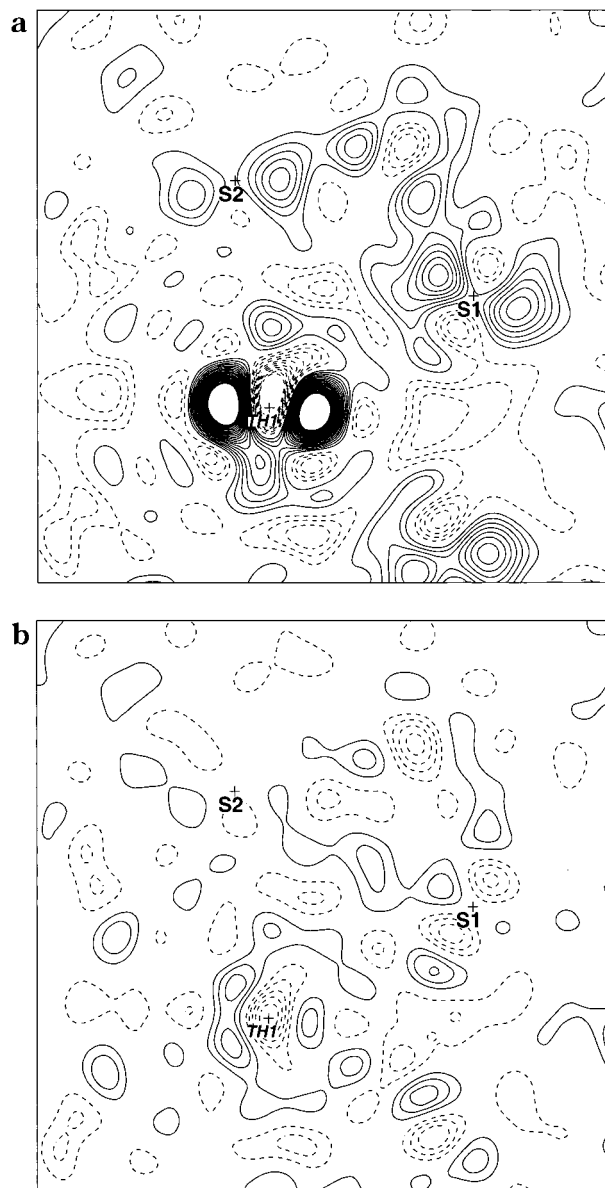


Figure 6. (a) Adjusted experimental deformation density. (b) Residual density in the Th-S(1)-S(2) plane.

theoretically 60.7 and 26.4° for this molecule. Thus the experiment shows some distortion toward a square antiprism, while the ab initio calculation gives a more perfect dodecahedron. The normalized bite of 1.14 , both observed and calculated, is in the range where we may expect some dodecahedral distortion toward a square antiprism in simple theoretical models.²² However, other experiments and our calculation suggest only small distortions. Experiment, our calculation, and simple theories show the Th-S(1) bond length is 1 or 2 percent longer than Th-S(2). The agreement between ab initio theory and experiment, given the large possible distortions, is acceptable, but the disagreement is significant both in angles and particularly in Th-S bond lengths. Some angular distortion and bond length compression may be due to the crystal packing forces, but the agreement of theory and experiment for tris-(acetylacetonato)ruthenium(III) is much better.²³ Thus there is some evidence that the Th-S bonding is not being calculated correctly.

(21) Kepert, D. L. *Inorganic Stereochemistry*; Springer-Verlag: Berlin, 1982.

(22) Bligh, D. G.; Kepert, D. L. *Inorg. Chem.* **1972**, *11*, 1556.

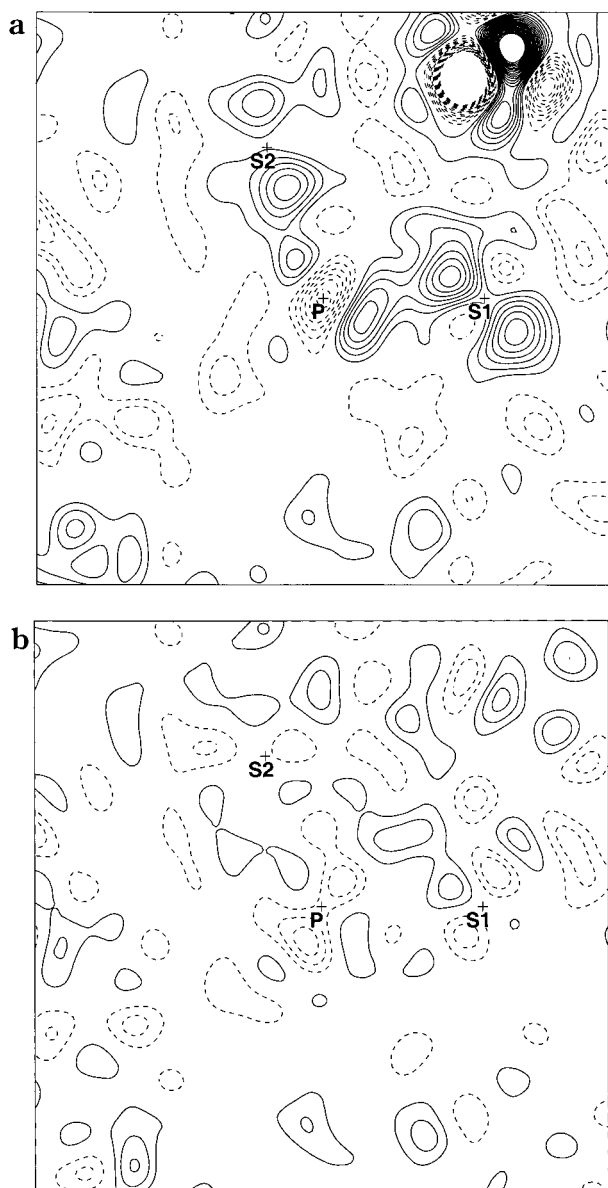


Figure 7. (a) Adjusted experimental deformation density. (b) Residual density in the S(1)–S(2)–P plane.

By contrast, the calculation of the dimethyldithiophosphinato geometry agrees very much better with experiment, even down to the geometry involving the smallest force constants—the methyl dihedral angles. This is, of course, expected, as such covalently bound lighter molecules are known to be well calculated by ADF. However, it is further evidence of weaker crystal packing forces and, thus, further points up the inadequacy in the calculation of the ThS₈ polyhedron geometry.

The molecular displacements at this temperature are dominated by zero-point vibrations of molecular internal modes. Figure 1 illustrates that they are qualitatively reasonable. The ratio of the thorium displacements to those for sulfur and phosphorus to those for carbon follow the expected (atomic mass)^{-1/2} ratios of 1:2.7:4.4 expected for zero-point motion well. The relative isotropy of thorium and phosphorus expected from the symmetric bonding environment is observed while the larger out-of-ThS₂P-plane amplitude for the sulfurs and the larger carbon amplitudes perpendicular to the P–C bond are also

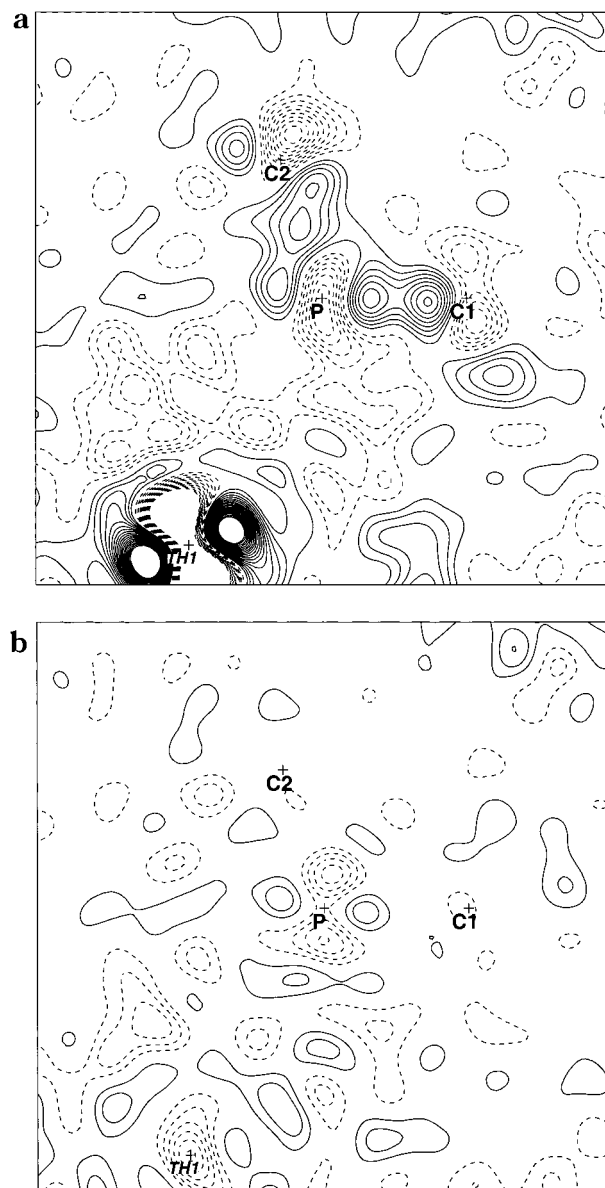


Figure 8. (a) Adjusted experimental deformation density. (b) Residual density in the P–C(1)–C(2) plane.

observed. These alignments of zero-point displacement ellipsoids, their relative sizes, and prolate/oblate/spherical nature are indicators that the whole refinement process is soundly based.

3.2. Molecular Electron Density. 3.2.1. Ligand Density.

The experimental deformation density maps in Figures 6a–8a show the pattern broadly expected in the deformation density of the ligand molecules. There are lone pair densities on both sulfurs and density maxima in all the S–P and P–C bonds. This is adequately modeled by second-order multipoles, the residual maps showing a significant defect only at the P site, where a dipolar hole remains. The bond maxima in the deformation density in the P–C bonds (0.5 and 0.8 e Å⁻³) are greater than those in the P–S bonds (0.3 and 0.5 e Å⁻³), which again exceed those in the density in the Th–S bonds (0.1 and 0.4 e Å⁻³). This is more clearly seen in the model density, and the relative sizes are reflected in the modeled bond overlap parameter values (P–C 0.95(14), 0.72(14); S–P 0.37(10), 0.45(11); Th–S 0.25(6), 0.22(6) electrons). Such differences, with P–C > P–S > Th–S, agree with previous measurements on bonding between first-row, second-row and metal ions. The

(23) Reynolds, P. A.; Cable, J. W.; Sobolev, A. N.; Figgis, B. N. *J. Chem. Soc., Dalton Trans.*, in press.

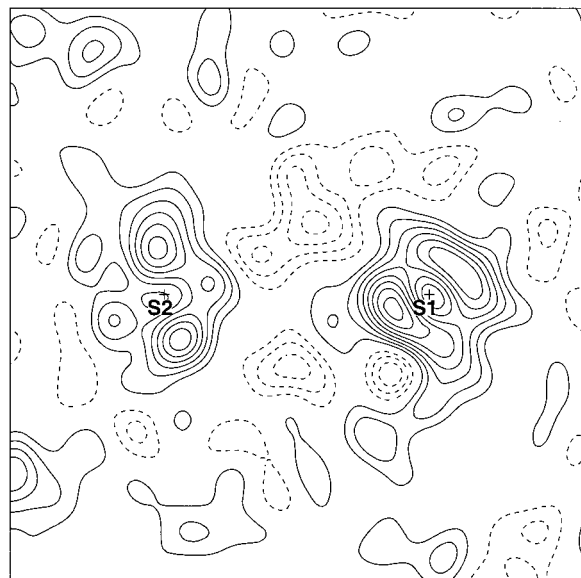


Figure 9. Adjusted experimental deformation density in the S(1)–S(2) plane perpendicular to the Th–S(1)–S(2) plane.

Table 3. Observed and Calculated Mulliken Atomic Charges

	ADF theory				exp
	L ⁻	(L ⁻) ₄	(4+)(L ⁻) ₄	ThL ₄	
Th				+1.23	+3.1(12)
S(1)	-0.69	-0.62	-0.49	-0.50	-0.9(3)
S(2)	-0.69	-0.62	-0.70	-0.50	-1.3(3)
P	+0.42	+0.89	+0.12	+0.80	+1.0(4)
C(1)H ₃	-0.02	-0.36	+0.12	-0.12	+0.2(5)
C(2)H ₃	-0.02	-0.31	+0.19	-0.12	+0.1(5)

overlap density in the Th–S bond is sufficiently close to the Th site and remote from S that it could be interpreted as thorium density, rather than overlap density, in contrast to the P–S and P–C densities, which are much more bond centered.

The lone pair densities on the two sulfurs are aligned approximately in the plane perpendicular to the ThS₂ plane. This causes some overlap with the P–S bond density maximum, from which it is not clearly separable. Figure 9 shows that this lone pair density is aligned within this plane differently on each sulfur. This alignment must be produced by the dodecahedral coordination to the thorium. The lone pair alignment on the dodecahedron produces a pattern which, perhaps, minimizes quadrupolar electrostatic interactions over the eight sulfur atoms or may be related to the noncoplanarity of Th, P, and the two S sites. The ThS₂ and PS₂ planes differ in angle by 9.5°. The phosphorus density shows accumulation of charge in the four bonds, depletion at the nucleus, and smaller depletion at a longer range away from the bond directions. This pattern is quite similar to that observed experimentally and reproduced theoretically in SO₄²⁻.⁵

Overall, the deformation density pattern on the dithiodimethylphosphinate ligand is as we expect, with only the lone pair orientation on the sulfurs indicating an obvious deviation from the free ligand density. Ab initio calculations to confirm this are beyond the scope of the present paper, which seeks to establish the reliability of the experiment and qualitative trends.

3.2.2. Thorium Density. We see a large anisotropic deformation on the thorium site. The likely reality of this is discussed in section 2.1. Figures 4a and 5a show a substantial depletion in density along *z* (–3.2 e Å⁻³) maximizing at 0.36 Å from the thorium site and an accumulation along [110] (+3.0 e Å⁻³) maximizing at a distance of 0.58 Å from the thorium.

We have successfully modeled this by use of the contracted d function as a deficit of 3.7(3) electrons in the *xz* + *yz* orbitals and an excesses in *xy* of 1.2(2) and in *x*² – *y*² of 3.5(2) electrons (compared to a spherical radon-like core). The radial dependence we have assumed is more contracted than that for Th 6d, corresponding better to Th 5d. We thus have experimental evidence for a charge polarization of the thorium core, mainly from *d*_{*xz*+*yz*} to *d*_{*x*²–*y*²}. In addition, the deformation maps show some in *ab* plane radial polarization and extra density, close to Th, in the Th–S vectors. The general lack of features in the residual maps shows that our model, essentially containing two full sets of fourth-order multipoles, can fit the deformation density. The residual map in the *ab* plane shows small features of height 0.3 e Å⁻³ which would require Th-centered functions of *f* symmetry (sixth-order multipole) to fit, but these are small. We can conclude that we see no significant diffuse density in the 6d or 5f region, either of *d* or *f* symmetry, but a very significant charge polarization in the core region of *d* symmetry. The lack of diffuse *f* or *d* bonding density suggests a quite ionic bonding situation, while the polarization suggests that the highest lying orbitals, 5d, in the Th⁴⁺ radon core, are not entirely innocent in the bonding, points to which we shall return.

It might be argued that the relatively icosahedral arrangement of sulfur sites around the thorium makes the observation of any *d* anisotropy on the thorium surprising. This might be so if only σ effects were involved. However, the further ligand environment is of only *D*₂ symmetry and, for instance, π bonding is only of tetrahedral symmetry for an idealized icosahedral sulfur arrangement. In addition, there is noticeable distortion even from this arrangement—for example, a P–Th–P angle of 106.58(2)° is observed, which is 2.89° less than that in an ideal tetrahedron. Such small distortions can have large ligand field and, thus, density effects.

The 3.3(5)% expansion of the core electron density as modeled may be significant—indicating a difference between the form factor calculation results and the thorium core in this crystal. The correlation with thermal parameters is small, and these are in any event too small to encompass this effect at these low temperatures. However, we should not ascribe this to a bonding effect, since equally valid explanations are systematic errors in the form factor calculation for this very heavy atom and in the experimental overall angular variation of observed intensities.

3.2.3. Covalence, Ionic Bonding, and Theory. Although the error is quite large, the net experimental thorium charge in Table 3 suggests an ionic bond, being close to +4. This supports our conclusions derived from the charge anisotropy on thorium. The net charges we observe—negative sulfur, positive phosphorus, and almost neutral methyl—are as predicted from simple chemical considerations of this ion, which we might consider on one side (S₂P=) to be a thiophosphate and on the other (=PMe₂) a phosphonium ion.

The ab initio calculations support this picture of ligand density. The free ligand has decidedly negative sulfurs and a +0.42 charge on the phosphorus. Assembly of four ligands polarizes the =PMe₂ half of the molecule to increase the phosphorus charge to +0.89 with negative methyl groups. Introduction of only the electrostatic part of the thorium removes this polarization completely. Last, introduction of the ab initio thorium center repolarizes the =PMe₂. However, it is also clear that the ab initio calculation is incorrect in giving a quite covalent wave function. The calculated thorium configuration is [radon core]6d^{1.35}f^{1.3} and quite anisotropic with the calculated *f* density varying from 0.32 e for *f*_{*xyz*} down to 0.07 for *f*_{*xxx*}. The

experiment shows none of this anisotropy and covalence. In addition, the large d-symmetry polarization of the core that is observed experimentally cannot be duplicated in this calculation, since the radon configuration thorium core is treated by the pseudopotential method and is thus *assumed* to be unpolarizable.

While the experiment is relatively convincing in assigning this compound as largely ionic, thus throwing doubt on the ADF result, there is related independent evidence to support this. An example is the measurement of the spin density by polarized neutron diffraction in UCl_4 .²⁴ The authors find less than 0.5% of the spin is delocalized onto each Cl site, although they do find substantial 5f–6d hybridization on the uranium site. We have been unable to successfully compute a stable wave function for the relevant UCl_8^{4-} cluster but have performed an analogous computation using ADF for the related ThCl_8^{4-} . Just as is calculated for our phosphinate complex, the first seven LUMOs are almost pure 5f split by ca. 3000 cm^{-1} . They each consist of 90–95% 5f, 0–2% 6d, and 5–10% chlorine Mulliken contributions. Thus, if we assume the uranium complex electron distribution is approximated by that of the thorium with two extra electrons in the f band, the ADF calculation would suggest that in the PND experiment we should see 5–10% of the spin on the chlorines and little d–f mixing. Thus in UCl_4 we also see the same contradiction between the covalent, small d–f mixed ADF wave function and the observation of ionicity and substantial d–f mixing. We are unaware of any other relevant diffraction experiments on insulating actinide compounds.

The general question of covalence in actinide complexes is not simple. There are the general principles that covalence is probably less important than in transition metals, and more than in the lanthanides, and that covalent effects are more important in lower oxidation states and earlier actinides. But, as exemplified in the qualified discussion of this topic by Cotton and Wilkinson,²⁵ experimental evidence for covalence in particular cases is mostly quite indirect (apart from the obvious exception

of the dioxo ions). This study shows that the most direct measure of covalence—charge transfer and electron distributions—can be usefully estimated by X-ray diffraction even in this most unfavorable of cases where actinide core electrons are present.

4. Conclusion

We have shown that, in this chemically relatively typical Th(IV) complex, the bonding is quite ionic with little diffuse f or d type density. Substantial polarization of the thorium ion is observed, but of d not of f symmetry. The polarization is found in the outer core region, revealing a 5d-like involvement in the bonding. ADF density functional calculations, in their present form, do not reproduce these observations. This suggests that, in general, theoretical calculations exaggerate the covalent nature of actinide bonds. It is the use of very low temperatures, much below those of liquid nitrogen, in combination with high-energy synchrotron radiation and area detection, which for the first time allows a direct characterization of actinide bonding through examination of electron distributions. With the increased data accuracy available at synchrotron sources, studies of compounds beyond the first transition series are now within reach.

Acknowledgment. B.B.I. and F.K.L. gratefully acknowledge support from the Carlsberg Foundation and a DANSYNC grant from the Danish Natural Science Research Foundation. This research was carried out in part at the National Synchrotron Light Source at Brookhaven National Laboratory, which is supported by the U.S. Department of Energy, Division of Materials Sciences and Division of Chemical Sciences. The SUNY X3 beamline at NSLS is supported by the Division of Basic Energy Sciences of the U.S. Department of Energy (Contract DEFG0286ER45231).

IC9715613

(24) Lander, G. H.; Brown, P. J.; Spirlet, M. R.; Rebizant, J.; Kanellakopoulos, B.; Klenske, R. *J. Chem. Phys.* **1985**, *83*, 5988.

(25) Cotton, F. A.; Wilkinson, G. *Advanced Inorganic Chemistry*, 5th ed.; Wiley: New York, 1988.